

Synopsis of
Minor Research Project

Principal Investigator

Harshkant O. Jethva

Physics Department, M. M. Science College,

Near Nazarbaug Railway Station, Dist: Rajkot

Morbi – 363642 (Gujarat)

Title of the Project: Growth and Characterization of Lead Tartrate Crystals

Objectives of the Project:

- (1) To grow lead tartrate crystals and some other possible tartrate crystals like Aluminum tartrate, Vanadium tartrate etc by gel method.
- (2) To grow mixed lead tartrate crystals like Pb – Cd mixed tartrate crystals, Pb – Co mixed tartrate crystals, Pb – Ag mixed tartrate crystals, Pb – Na mixed tartrate crystals, Pb – Fe mixed tartrate crystals, Pb – Ni mixed tartrate crystals, Pb – K mixed tartrate crystals.
- (3) To characterize the grown crystals by different techniques like FTIR, XRD, EDAX and TGA.

1. Introduction

Systemic study of the growth and properties of crystals is covered under the subject of crystal growth. The growth of crystals in the crust of Earth is the natural minerals and often considered as precious stone. However, due to the development of modern science and technology, it is possible to synthesize and grow several varieties of crystals in the laboratory also. This has brought the field of crystal growth into the limelight. The crystals have many applications such as harmonic frequency generators, polarizer, piezo-electric devices, holographic devices, substances for thin film, laser devices, magnetic devices, detection as well as data storage devices etc. For various applications of crystals in the field of science and technology, there always has been a requirement for good quality crystals and hence, various growth techniques developed to grow suitable crystals.

The subject of crystal growth in gel is not new. It has enjoyed at least two long periods of popularities, one during the second half of 1800 and second roughly during the period 1913 – 1926. The gel growth technique is elaborately described by Henisch¹,

Henisch et al² as well as Patel and Rao³. This is quite simple but an important technique. This technique is well suited for the crystal growth of compounds, which are sparingly soluble and decomposed at fairly low temperatures. This technique can be set up in a laboratory with simple glasswares and without any need of sophisticated instruments and high temperature furnaces. By carefully selecting the gel density, pH and concentration of the reactants, good quality crystals can be grown at room temperatures. Even today, the gel growth technique continues to attract various researchers. The present work deals with the growth of tartrate crystals by gel technique.

Several tartrate compounds have various applications in various fields. For example, injections of Na – Cr tartrate, Na – Fe (III) tartrate and K – Cr tartrate increase the susceptibility of transplanted sarcoma to the effect of X – rays. Tartrate salt compound is used to prevent cognitive disorders associated with diabetes⁴. The prostate cancer is treated with tartrate ions⁵. Certain tartrate compounds find applications in the field of cosmetics. For example, diacetyl tartrate of fatty acid glycerides is used as hair conditioner additive⁶. The tanning action of iron tartrate to tan skin is also reported⁷. There are also other numerous applications of compounds of tartrate in the field of science and technology. For example, ferroelectric applications of sodium - potassium tartrate⁸ and calcium tartrate⁹, ferroelectric-ferroelastic applications of sodium - ammonium tartrate¹⁰ and dielectric applications of lithium thallate tartrate¹¹. Manganese tartrate crystals being temperature sensitive can be used to sense and measure temperature. There are certain industrial applications of different tartrate compounds. Zinc tartrate with other compounds form a bright coating and protecting powder for metals¹². Antimony tartrate can be used as a corrosion inhibitive composition for coolant

systems¹³. Calcium tartrate crystals show many properties such as ferroelectric, dielectric, optical and thermal properties¹⁴. Various important applications of different tartrate crystals in different fields have led the present author to grow tartrate crystals.

2. Experimental Techniques

2.1 Gel Preparation

AR Grade sodium metasilicate powder was used to prepare gel medium. In a beaker, 250 gram sodium metasilicate was dissolved in one liter of distilled water. On stirring it thoroughly, dense milky solution of sodium metasilicate was formed. It was left for a couple of days, so that heavy insoluble impurities accumulate at the bottom of the beaker. This was decanted into another beaker and filtered twice with Whatman (cat no 1001 125) filter paper of 12.5 cm diameter. Then solution was centrifuged on MSE high speed centrifuge unit for about half an hour at 1000 rpm. Practically, all suspended impurities were got rid off and as a result transparent golden colored solution of sodium metasilicate was obtained. The specific gravity of the solution was chosen 1.04.

Then AR Grade levo tartratic acid powder was used to prepare 1 M solution. It was mixed with the solution of sodium metasilicate in such a way that the pH of the mixture was maintained 4.5.

By measuring cylinder, 15 ml of mixture was taken into test-tube. The mixture was poured into test-tube in such a way that there should not present any air bubble. After some days, semi solid in nature, stable in form and flexible medium was obtained due to the interaction of the compound used to prepare the mixture, which is known as gel.

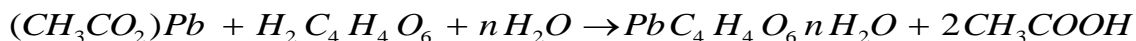
2.2 Crystal Growth

The objectives of the project are to grow lead tartrate and mixed lead tartrate crystals. To grow lead tartrate crystals, AR Grade lead acetate powder was used to prepare 1 M solution. After setting the gel, this supernatant solution was gently poured in the test-tube without disturbing the gel surfaces.

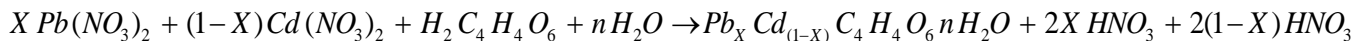
To grow the mixed lead tartrate crystals, AR Grade lead nitrate powder was used to prepare 1 M solution. Similarly, AR Grade cadmium nitrate, copper nitrate, silver nitrate, sodium nitrate, ferrous nitrate, nickel nitrate, potassium nitrate and ammonium nitrate powder were used to prepare 1 M solution of each. After setting the gel, the supernatant solutions consisting of (6 ml lead nitrate + 4 ml cadmium nitrate), (6 ml lead nitrate + 4 ml copper nitrate), (6 ml lead nitrate + 4 ml silver nitrate), (6 ml lead nitrate + 4 ml sodium nitrate), (6 ml lead nitrate + 4 ml ferrous nitrate), (6 ml lead nitrate + 4 ml nickel nitrate), (6 ml lead nitrate + 4 ml potassium nitrate) and (6 ml lead nitrate + 4 ml ammonium nitrate) were gently poured in the test-tubes without disturbing the gel surfaces.

The following reactions were expected to occur.

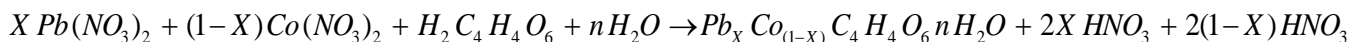
(1) The expected reaction for lead tartrate crystals was



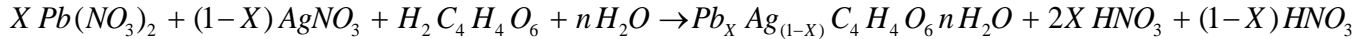
(2) The expected reaction for Pb – Cd mixed tartrate crystals was



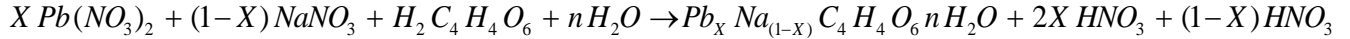
(3) The expected reaction for Pb – Co mixed tartrate crystals was



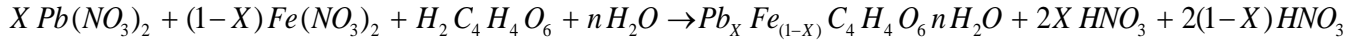
(4) The expected reaction for Pb – Ag mixed tartrate crystals was



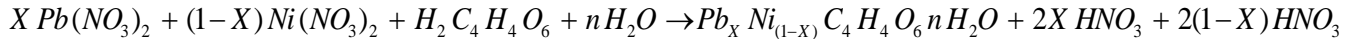
(5) The expected reaction for Pb – Na mixed tartrate crystals was



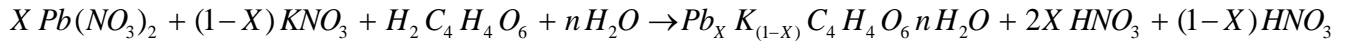
(6) The expected reaction for Pb – Fe mixed tartrate crystals was



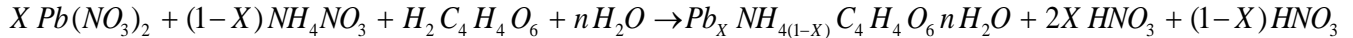
(7) The expected reaction for Pb – Ni mixed tartrate crystals was



(8) The expected reaction for Pb – K mixed tartrate crystals was



(9) The expected reaction for Pb – NH₄ mixed tartrate crystals was



In all the equations $X = 0.6$

2.3 Crystal Growth observation

The different supernatant solutions were poured in such a way that the total volume of the supernatant solutions remained constant. The following observations were noted nearly one month after pouring supernatant solutions on the set gel. The crystal growth observations were made for pH 4.5 and gel density of 1.04 gm/cc.

2.3.1 For supernatant solution lead acetate, there were small crystals available in gel liquid interface. Away from the gel liquid interface, some crystals were found long and some were found short in length. The color of the crystals was off white. Figure 1 shows this type of crystal growth.

2.3.2 For supernatant solution lead nitrate and cadmium nitrate, there were small crystals were grown at the gel liquid interface. Below the gel liquid interface, there were many irregular shaped crystals, arranged in the row were shown. The color of the crystals was

nearly white. Near the bottom of the test tube, two or three irregular shaped crystals were found. Figure 2 shows this type of growth.

2.3.3 For supernatant solution lead nitrate and cobalt nitrate, there were small crystals available in gel liquid interface. Away from the gel liquid interface, some crystals were found nearly equal in length. The color of the solution was radish and the color of the crystals was nearly white. Figure 3 shows this type of crystal growth.

2.3.4 For supernatant solution lead nitrate and silver nitrate, small crystals in large quantity were seen at the gel liquid interface. As we move just away from the interface, the crystals were separated out but they were arranged in the circular shape in the plane of the test tube. More away from the interface, crystals were more separated out in irregular manner. Near the bottom of the test tube, nearly ten small crystals were found. The crystals were white in color. Figure 4 shows this type of growth.

2.3.5 For supernatant solution lead nitrate and sodium nitrate, yellowish solution is obtained and whole test tube was found cloudy. No crystals were separately seen. The color of the sample was yellowish white. Figure 5 shows this type of growth.

2.3.6 For supernatant solution lead nitrate and ferrous nitrate, yellowish solution was obtained. No crystals were found at the interface. Away from the interface, irregular shaped, large quantity crystals were obtained. The color of the crystals was yellowish white. Figure 6 shows this type of growth.

2.3.7 For supernatant solution lead nitrate and nickel nitrate, white colored large amount of crystals were grown at the gel liquid interface. No crystals were found near the bottom of the test tube. Figure 7 shows this type growth.

2.3.8 For supernatant solution lead nitrate and potassium nitrate, white colored and granule type crystals were found at the gel liquid interface. No crystals were found near the bottom of the test tube. Figure 8 shows this type of growth.

2.3.9 For supernatant solution lead nitrate and ammonium nitrate, white colored irregular shaped crystals were found from the interface up to half of the gel medium. No crystals were found at the bottom of the test tube. Figure 9 shows this type of growth.



Fig. 1. Lead Tartrate



Fig. 2. Pb – Cd mixed Tartrate



Fig. 3. Pb – Co mixed Tartrate



Fig. 4. Pb – Ag mixed Tartrate



Fig. 5. Pb – Na mixed Tartrate



Fig. 6. Pb – Fe mixed Tartrate



Fig. 7. Pb – Ni mixed Tartrate

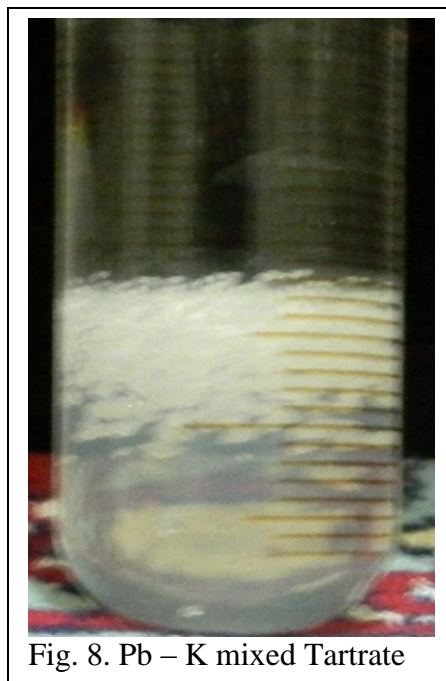


Fig. 8. Pb – K mixed Tartrate

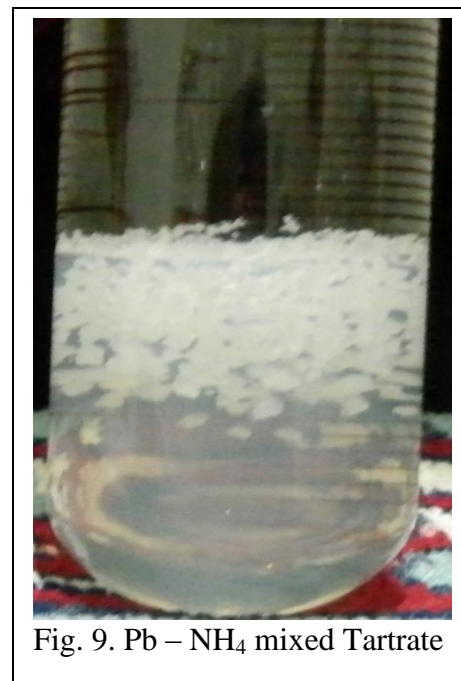


Fig. 9. Pb – NH₄ mixed Tartrate

3. Characterization of the Crystals

3.1 Characterization of Lead Tartrate Crystal

3.1.1 FTIR Spectroscopy study

FTIR spectrum of the grown crystals was recorded in the wave number range 4000 – 400 cm⁻¹. Figure 10 shows the FTIR spectra for the lead tartrate crystals.

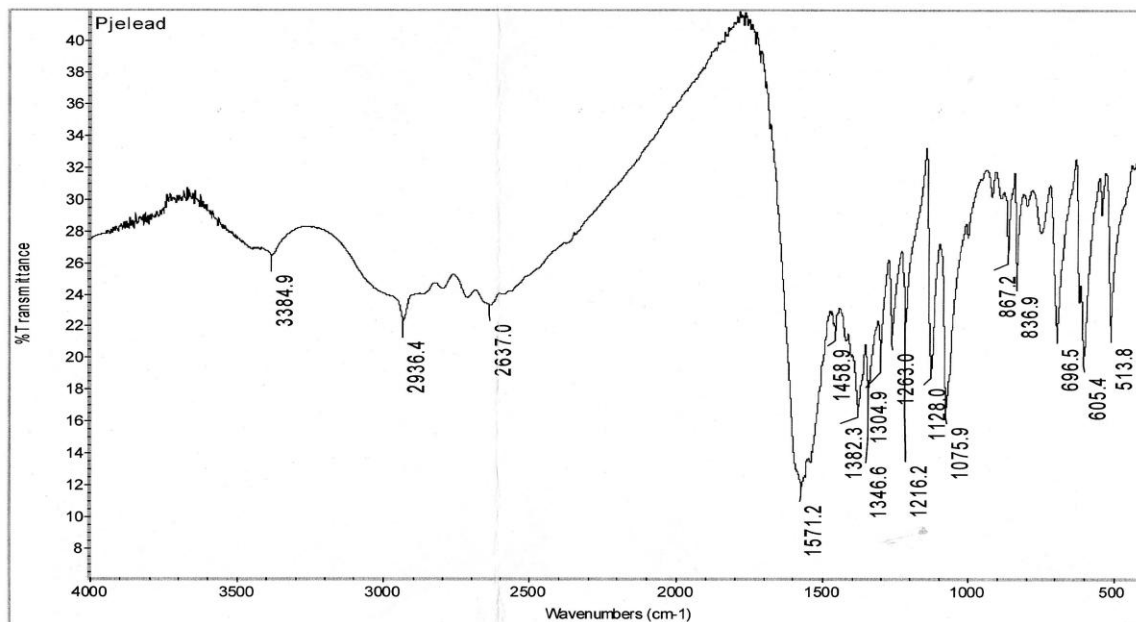


Figure 10: FTIR spectrum

It is observed that absorption occurring around 3400 cm^{-1} is due to the asymmetric and symmetric stretching of O – H bond, which generally indicates the presence of water of crystallization. The absorption occurring around 1600 cm^{-1} corresponds to the carboxyl (C = O) group stretching. The absorption occurring at around 1385 cm^{-1} is due to C – O stretching vibration. The peak at $1128\text{--}1075\text{ cm}^{-1}$ is due to C – O stretching of (–COO–). Absorptions around 1075 cm^{-1} , 867 cm^{-1} and 836 cm^{-1} are due to the O – H stretching out of plane vibrations, while the absorption from 900 cm^{-1} to 513 cm^{-1} are due to the metal oxygen bond.

3.1.2 Powder X – ray diffraction (XRD) Study

In this investigation an attempt is made to find out the unit cell parameters of lead tartrate crystals using powder – x computer program, h , k and l parameters as well as d and 2θ values are generated in such a way that these values match with the X – ray powder diffraction values.

Figure 11 shows the powder XRD pattern of the lead tartrate crystals.

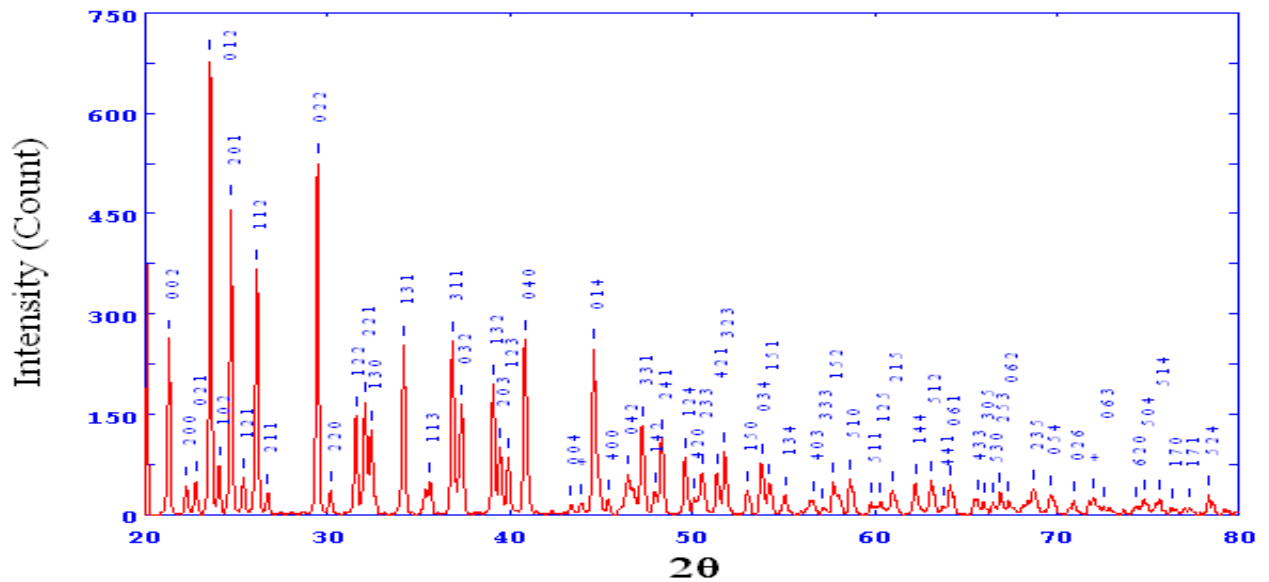


Figure 11: The Powder XRD pattern for lead tartrate crystal

The values of 2θ , (h, k, l) , d and relative intensities of the XRD patterns are tabulated in the following table1.

2θ degree	Relative Intensity (%)	d (A°)	(h, k, l)
21.310	262.80	4.16939	(0 0 2)
23.575	680.94	3.77370	(0 1 2)
24.719	463.31	3.60154	(2 0 1)
26.129	367.13	3.41035	(1 1 2)
29.446	526.56	3.03326	(0 2 2)
34.182	253.49	2.62308	(1 3 1)
36.857	260.51	2.43859	(3 1 1)
40.824	262.11	2.21031	(0 4 0)
44.595	247.99	2.03178	(0 1 4)

Table1: Powder X – ray diffraction data of lead tartrate crystals

From the powder XRD studies it was found that the lead tartrate crystal has orthorhombic crystal structure with unit cell parameters $a = 7.99482$, $b = 8.84525$ and $c = 8.35318$.

3.1.3 Thermal study

Figure 12 shows the thermogram of the lead tartrate crystal.

The graph shows that the sample is stable from room temperature to approximately 220° C. Then rapid decomposition starts up to 550° C. After this temperature a very small loss of weight is noticed.

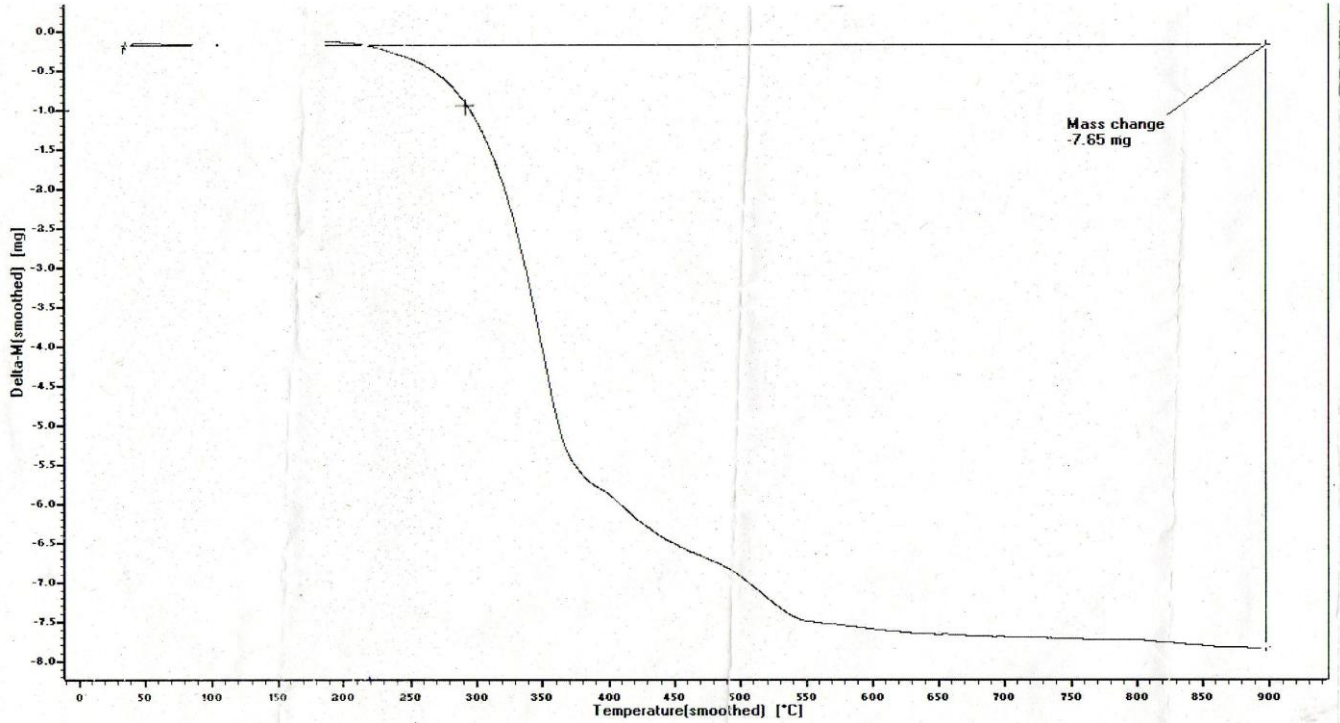


Figure 12: Thermogram of lead tartrate crystal

3.1.4 Kinetic and thermodynamic study of dehydration

Usually, the kinetic parameters can be evaluated from the TG curves by applying several equations which are proposed by different authors on the basis of different assumptions to the kinetics of the reaction and the Arrhenius law. These equations are (1) the Coats and Redfern relation (2) the Horowitz and Metzger relation and (3) the Freeman and Corroll relation. In the present investigation the Coats and Redfern relation is discussed.

This relation facilitates to evaluate the activation energy, order of reaction and frequency factor. Coats and Redfern (C – R) relation

$$\text{is } \log_{10} \left(\frac{1 - (1 - \alpha)^{1-n}}{T^2(1-n)} \right) = \log_{10} \left(\frac{AR}{\alpha E} \right) \left(1 - \frac{2RT}{E} \right) - \frac{E}{2.3RT}$$

In this equation E is the activation energy of the reaction, A is the frequency factor, α is the fraction of decomposed material at time t, n is the order of reaction and T is the absolute

temperature. The plots of $y = \log_{10} \left(\frac{1 - (1 - \alpha)^{1-n}}{T^2(1-n)} \right)$ versus $x = \frac{1}{T}$ were straight line for

different values of n , however, the best linear fit curve gives the correct value of n . This

was found for $n = \frac{3}{4}$. Figure 13 shows the plot drawn for Coats Redfern relation. The

values of different kinetic parameters obtained from the C-R relation are shown in the

following table 2.

Order of reaction (n)	Activation energy (E)	Frequency factor (A)
3/4	67.84 kJ/mol	3.631×10^{17}

Table 2: Different Kinetic Parameters

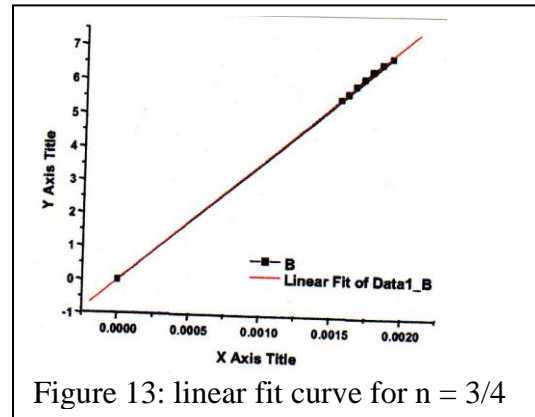


Figure 13: linear fit curve for $n = 3/4$

The values of different thermodynamics parameters such as, the standard entropy of activation ($\Delta^\#S^\circ$), standard enthalpy ($\Delta^\#H^\circ$), standard Gibbs free energy ($\Delta^\#G^\circ$) and standard change in internal energy ($\Delta^\#U^\circ$) were calculated by applying well known formula, are shown in the following table 3.

Standard Entropy ($\Delta^\#S^\circ$)	Standard Enthalpy ($\Delta^\#H^\circ$)	Standard Gibbs free Energy ($\Delta^\#G^\circ$)	Standard change in Internal energy ($\Delta^\#U^\circ$)
0.086 kJ/mol	58.4 kJ/mol	10.2 kJ/mol	63.16 kJ/mol

Table 3: Different Thermodynamics Parameters

From the table 3, it can be noticed that standard entropy of activation ($\Delta^\#S^\circ$) and standard enthalpy of activation ($\Delta^\#H^\circ$) are positive and suggest that the process is spontaneous at

high temperatures. Positive value of standard Gibbs free energy ($\Delta^{\#}G^{\circ}$) suggests that the sample is thermodynamically unstable.

3.2 Characterization of Pb – Cd mixed Tartrate crystal

3.2.1 FTIR Spectroscopy Study

FTIR spectrum of the grown crystals was recorded in the wave number range 4000 – 400 cm^{-1} . Figure 14 shows the FTIR spectra for the Pb – Cd mixed tartrate crystals. It is observed that the absorption occurring round about 1600 cm^{-1} corresponds to the carboxyl (C = O) group stretching. The absorption occurring at round 1385 cm^{-1} is due to C – O stretching vibration. The peak at 1128-1075 cm^{-1} is due to C – O stretching of (-COO-). Absorptions around 1005 cm^{-1} , 867 cm^{-1} and 836 cm^{-1} are due to the O – H stretching out of plane vibrations, while the absorption from 900 cm^{-1} to 513 cm^{-1} are due to the metal oxygen bond.

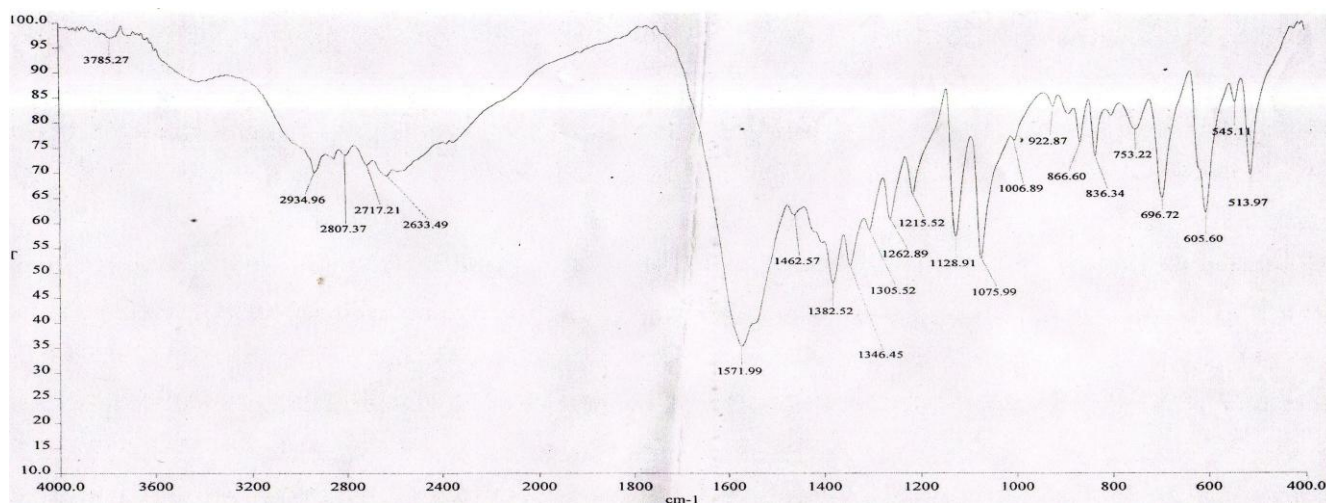


Figure 14: FTIR spectrum

3.2.2 Powder X – ray diffraction (XRD) Study

Here an attempt is made to find out the unit cell parameters of Pb – Cd mixed tartrate crystals using powder – x computer program, h , k and l parameters as well as d and 2θ values are generated in such a way that these values match with the X – ray powder diffraction values.

Figure 15 shows the powder XRD pattern of the lead tartrate crystals.

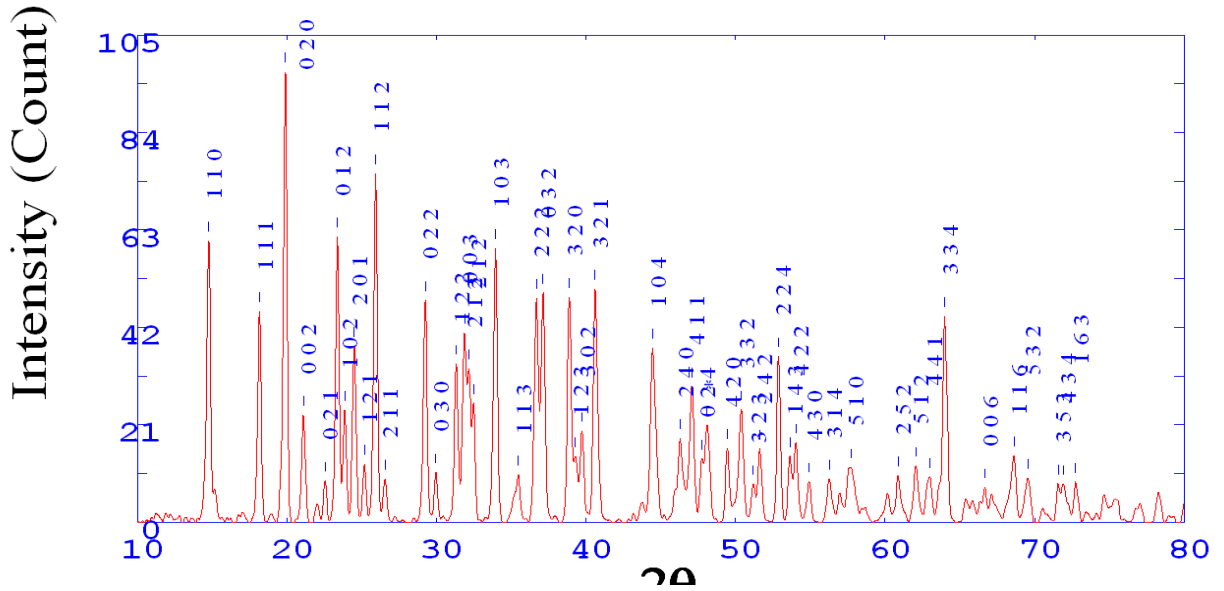


Figure 15: The Powder XRD pattern for Pb – Cd mixed tartrate crystal

The values of 2θ , (h, k, l) , d and relative intensities of the XRD patterns are tabulated in the following table 4.

2θ degree	Relative Intensity (%)	d (Å°)	(h, k, l)
14.773	60.68	5.99611	(1 1 0)
18.163	45.41	4.88400	(1 1 1)
19.897	97.14	4.46222	(0 2 0)
23.375	61.51	3.80550	(0 1 2)

25.926	75.16	3.43654	(1 1 2)
29.251	47.81	3.05307	(0 2 2)
33.947	59.02	2.64067	(1 0 3)
40.609	50.25	2.22151	(3 2 1)
44.455	37.57	2.03785	(1 0 4)

Table 4: Powder X – ray diffraction data of Pb – Cd mixed tartrate crystals

From the powder XRD studies it was found that the Pb – Cd mixed tartrate crystal has orthorhombic crystal structure with unit cell parameters $a = 8.124$, $b = 8.94$ and $c = 8.42$.

3.2.3 Thermal Study

Figure 16 shows the thermogram of the Pb – Cd mixed tartrate crystal.

The graph shows that the sample starts to decompose rapidly from room temperature to approximately 150° C. Then it becomes nearly stable up to approximately 280° C. Again rapid decomposition starts up to 450° C. After that the sample loses its mass at stable rate approximately 0.4% per 50 °C up to 900° C.

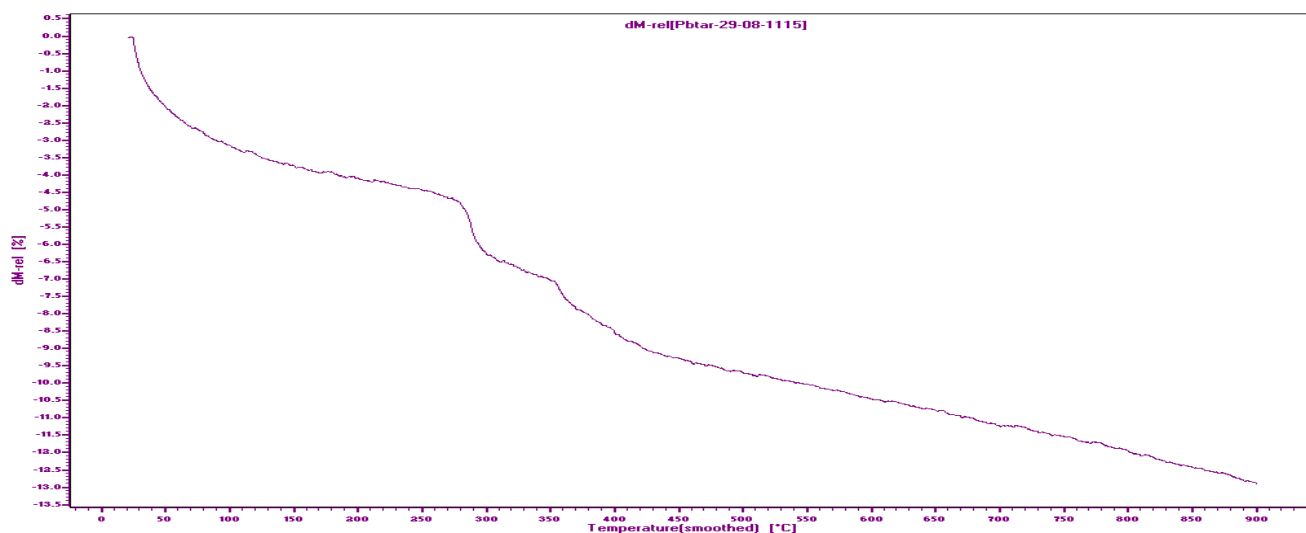


Figure 16: Thermogram of Pb – Cd mixed tartrate crystal

3.2.4 Kinetic and thermodynamic study of dehydration

As discussed above, the kinetic parameters were evaluated from the TG curves by

applying the Coats and Redfern relation. The plots of $y = \log_{10} \left(\frac{1 - (1 - \alpha)^{1-n}}{T^2 (1-n)} \right)$ versus

$x = \frac{1}{T}$ were straight line for different values of n, however, the best linear fit curve gives

the correct value of n. This was found for $n = \frac{5}{2}$. Figure 17 shows the plot drawn for

Coats Redfern relation. The values of different kinetic parameters obtained from the C-R

relation are shown in the following table 5.

Order of reaction (n)	Activation Energy (E)	Frequency factor (A)
5/2	16.495 kJ	1.97×10^{11}

Table 5: Different Kinetic Parameters

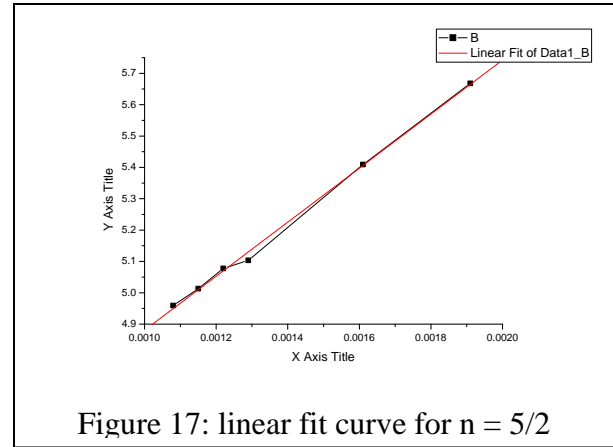


Figure 17: linear fit curve for n = 5/2

The values of different thermodynamics parameters such as, the standard entropy of activation ($\Delta^\#S^\circ$), standard enthalpy ($\Delta^\#H^\circ$), standard Gibbs free energy ($\Delta^\#G^\circ$) and standard change in internal energy ($\Delta^\#U^\circ$) were calculated by applying well known formula, are shown in the following table 6.

Standard Entropy ($\Delta^\#S^\circ$)	Standard Enthalpy ($\Delta^\#H^\circ$)	Standard Gibbs free Energy ($\Delta^\#G^\circ$)	Standard change in Internal energy ($\Delta^\#U^\circ$)
0.156 kJ/mol	6.136 kJ/mol	- 91.332 kJ/mol	11.316 kJ/mol

Table 6: Different Thermodynamics Parameters

From the table 6, it can be noticed that standard entropy of activation ($\Delta^\ddagger S^\circ$) and standard enthalpy of activation ($\Delta^\ddagger H^\circ$) are positive and suggest that the process is spontaneous at high temperatures. Negative value of standard Gibbs free energy ($\Delta^\ddagger G^\circ$) suggests that the chemical reaction proceeds spontaneously in forward direction.

3.2.5 EDAX Study

In order to find out elemental composition of the grown crystal, the EDAX is employed here. The EDAX spectra of the Pb – Cd mixed tartrate crystal is shown in the figure 18.

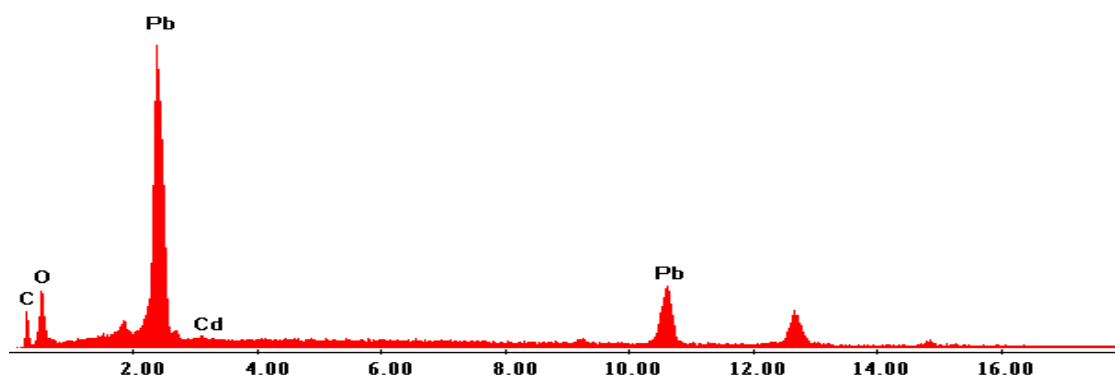


Figure 18: EDAX spectra of Pb – Cd mixed tartrate crystals

It is found from the figure 18 that the elemental contribution of C and O is due to the tartrate ions and water of hydration. It is also clear from the figure 18 that the atomic percent of Pb is very high compared to Cd which is due to the incomplete filled orbital of Pb and completely filled orbital of Cd. The proposed formula and estimated formula for the sample are $\text{Pb}_{0.6} \text{Cd}_{0.4} \text{C}_4 \text{H}_4 \text{O}_6 \cdot n\text{H}_2\text{O}$ and $\text{Pb}_{0.7401} \text{Cd}_{0.003} \text{C}_4 \text{H}_4 \text{O}_6 \cdot n\text{H}_2\text{O}$ respectively.

Scope for the future work: The future work in continuation with the present work may be pursued as follows.

The effect of various tartratic acids (dextro and levo) in the composition of crystals can be studied. This will enable the researcher to identify the effect of dextro and levo rotator tartaric acid in the crystalline compounds. As mentioned above, the author has developed some mixed tartrate crystals with Pb In future; there is a scope for carrying out the dielectric, powder XRD, FTIR, TGA and EDAX studies of all the developed tartrate crystals. Further, by varying the composition of the supernatant solutions, one can develop the mixed tartrate crystals and can be analyzed by different techniques.

General References

1. H. K. Henisch; "Crystal Growth in Gels" Dover Publication, New York, (1993)
2. H. K. Henisch, J. Denny and H. I. Hanoka; Chem. Solids, **26** (1965) 493.
3. A. R. Patel and A. V. Rao; J. Cryst. Growth, **43** (1978) 351.
4. N. H. Greig, United States Patent, 60105940, (2006)
5. Lebioda, United States Patent, 5763490, (1998)
6. Leidreiter, et al, United States Patent, 5750097, (1998)
7. M. Kubota; J. Chem. Soc., Japan, Ind. Chem Sect., **57** (1954) 594.
8. J. Valasek; Phys. Rev., **17** (1921) 475.
9. H. B. Gon; J. Cryst. Growth., **102** (1990) 501.
10. K. Aizu; J. Phy. Soc., Pap., **31** (1971) 1521.
11. E. Sawaguchi and L. E. Cross; Ferroelectrics, **2** (1971) 37.
12. M. A. Rossi; Patent no. 581, 803, Ital, 9th Sept., (1958)
13. N. E. Payerle, United States Patent, 4686059, (1987)
14. X. SahayaShajan and C. Mahadevan; Cryst. Res. Technol., **40**, 598.